The following supplements accompany the article

Gray whale densities during a seismic survey off Sakhalin Island, Russia

Judy E. Muir*, Laurie Ainsworth, Roberto Racca, Yury Bychkov, Glenn Gailey, Valeriy Vladimirov, Sergei Starodymov, Koen Bröker

*Corresponding author: jemuir@telus.net

Endangered Species Research 29: 211–227 (2016)

Supplement 1: The information contained in this Supplement provides details of methods used to estimate gray whale density surfaces.

Each scan at an observation station sampled a semicircular area surrounding that station. The 0.1 reticle distance limit for a scan's coverage at a station was chosen as a compromise between increasing the shore-based survey coverage for the density analysis as much as possible, while recognizing the uncertainty in assigning a sighting at zero reticles to a particular grid cell. ArcGIS v 10.1 (ESRI 2012) was used to create 0.1 reticle distance buffers for each sampled station, overlay them on the grid cell surface, and calculate the area of each covered grid cell.

Density estimates applied corrections for availability and detection bias that result in an underestimation of animal abundance (Marsh & Sinclair 1989). The availability correction ($\hat{a}$), i.e., the probability that a gray whale was on the ocean surface and available to be detected, was estimated based on the portion of time, and hence the probability, that a whale was on the ocean surface while an observer was scanning that particular patch of water (McLaren 1961). The time a patch of water was in view was estimated using the Fujinon 7x50 binoculars 7°30' field of view and the observer scanning rate. Gray whale surface time was estimated using gray whale dive cycle time collected in the field (Gailey et al. 2011). The availability correction was estimated separately for behaviour and distribution scans due to small differences in scanning rates.

Conventional distance sampling methods could not be used to analyze the effects of distance and other covariates on the probability of detecting an available gray whale ($\hat{p}$) because the gray whale density gradient with respect to shore violates one of the main assumptions that objects are distributed uniformly with respect to distance in any direction from the sampling point (Buckland et al. 2001). Instead, we conducted a double platform (vessel and shore-based) experiment in 2006 to estimate the shore-based detection function. The model to estimate parameters of a shore-based detection function included both the shore-based and ship-based sightings in a joint analysis. This analysis indicated the detection function was flat (i.e., detection did not decrease with increasing distance from the observer), up to the 8 km distance tested (Rexstad & Borchers unpubl.). Effects of environmental covariates on detection probability were not tested in the double-platform analysis due to small sample sizes.

LITERATURE CITED

Buckland ST, Anderson DR, Burnham KP, Laake JL, Borchers DL, Thomas L (2001) Introduction to distance sampling: estimating abundance of biological populations. Oxford University Press, Oxford, UK

ESRI (2012) ArcGIS software products. Environmental Systems Research Institute Redlands, CA

Gailey G, Sychenko O. Würsig B (2011) Patterns of western gray whale behavior, movement, and occurrence off Sakhalin Island, 2010. Chapter 4 in: Western gray whale research and monitoring program in 2010, Sakhalin Island, Russia. Volume II results and discussion. Prepared for Exxon Neftegas Limited and Sakhalin Energy Investment Company Limited, Yuzhno-Sakhalinsk, RU p 286–348. Available at: http://cmsdata.iucn.org/downloads/wgwap_10_doc_14_2010_mnr_report_volume_ii_results___eng___reducedsize.pdf (accessed 5 September 2013)

McLaren IA (1961) Methods for determining the numbers and availability of ringed seals in the eastern Canadian Arctic. Arctic 14, 162–175

Marsh H, Sinclair DF (1989) Correcting for visibility bias in strip transect aerial surveys of aquatic fauna. J Wildl Manage 53:1017-1024

Supplement 2: The information contained in this Supplement provides details of methods used to calculate sound covariates.

Initial model building suggested the need for complex interaction and polynomial terms for grid cell centroid eastings and northings. Two categorical variables were created at the grid cell level to capture a large amount of the information regarding the magnitude of sound exposure (ensonification level) and the pattern of sound exposure as the seismic vessel sailed past a point when the airguns were firing (ensonification pattern). These summary variables provided a simple representation of the complex interaction terms and allowed simpler models to be developed for assessing responses of densities to sound.

The ensonification level category was determined by binning grid cell sound accumulations in 10 dB increments (a balance between accuracy and simplicity) and mapping each of the 3 hr, 3 d and 7 d cumulative sound exposure level (cSEL) covariates on days 2, 7, 10, 12 and 14 of the seismic survey. A consistent pattern of ensonification level was observed. We used cut points at 165 and 175 dB re 1 μPa^2-s for 3 d cSEL on day 10 to classify each grid cell into one of three ensonification level categories with approximately equal sample size.

We selected six grid cell centroids in shallow and deep water in the northern, central and southern parts of the study area to explore patterns in sound exposure from the airguns (Fig. S1). We classified cells into three different ensonification patterns depending on the cell's relative position to the line being sailed by the seismic vessel while the airguns were being fired and the vessel's sailing direction (Fig. S2). Cells entirely to the north or south of the seismic area experienced monotonic increases and decreases in sound exposure, and were assigned to a "north" and "south" category respectively. Cells adjacent to the "bulges" at the north and south ends of the seismic survey area experienced either an inverted "V" or monotonic pattern of sound depending on the seismic line being shot. These cells were also assigned to the "north" and "south" categories. The remaining cells had a well defined inverted "V" pattern of sound exposure and were assigned to a third "central" category (Fig. S3).

We used Functional Principal Components Analysis (FPCA; Ramsay & Silverman 2005) to create a small number of variables that captured the majority of survey to survey differences in cSEL across the time series at all grid cell centroids in the 3 hr, 3 d and 7 d time windows. The survey level cSEL series in each time window were represented as curves using b-splines. A curve in a 3 hour time window typically only needed to accommodate a couple of 'jump' points where the sound transitioned from "on" to "off" or vice versa because the seismic vessel required ~2 hr to sail a transect line (when airguns were firing) or to complete a turn between lines (when airguns were silent). Conversely, a 3 d or 7 d time window spanned the sailing of several seismic lines, resulting in multiple jumps between on and off sound that were not well captured by b-splines. We therefore calculated two sets of FPCA covariates for each of the 3 d and 7 d windows by smoothing the five minute time series using 8–hr averages, and again with 24–hr averages. The two sets of FPCs for each time window thus captured differences in the shape of the 8–hr or 24–hr means in sound within the time window.

The first three FPCs for the 3 d FPCA using an 8–hr smooth accounted for a total of 65% of the survey to survey variation in 8 hr sound. However, these FPCs were not particularly useful as they did not seem to capture meaningful summaries of the data. For example, although the first FPC captured high sound at the beginning and end of the time interval (40% of the total variation), the second and third FPCs captured high sound at very localized points in the time window (13% and 11% of total variation) and did not render meaningful interpretations.

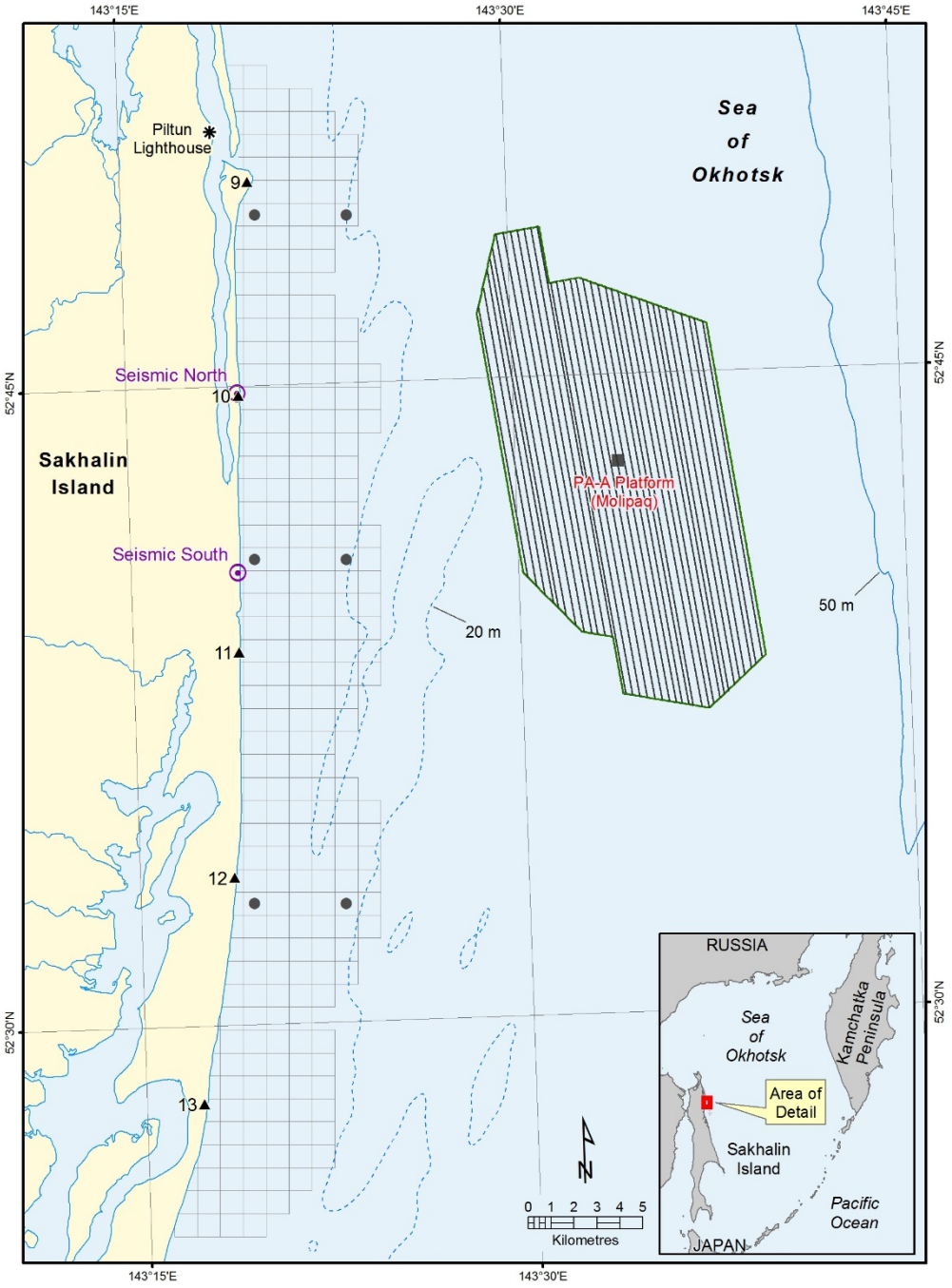

Fig. S1. Study area and grid cell coverage for the southern distribution (triangles) and behaviour (squares) shore-based stations that conducted gray whale scans used to estimate densities. The six grid cell centroids that were used to explore patterns in the airgun sound are illustrated as black circles. Estimated 20 m and 50 m bathymetry contours are shown as light and dark blue lines respectively.

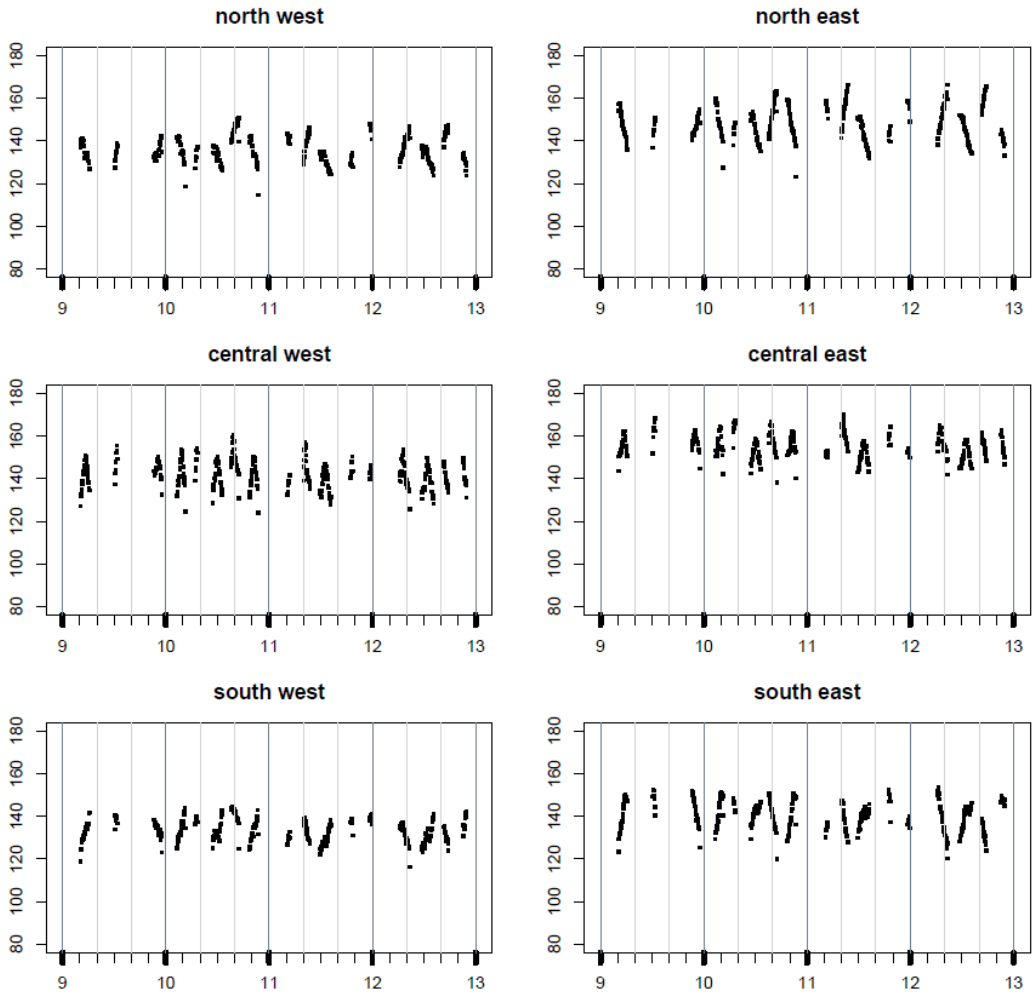

Fig. S2. Patterns of seismic cSEL in dB re 1 μPa^2-s over 5 minute bins at the six representative grid cell centroids during 26 to 30 June 2010 (days 9 to 13 of the seismic survey). The north and south points show opposite patterns of monotonic increases or decreases in 5 minute sound exposure as the seismic vessel sailed by while firing the airgun array. Central points show an inverted "V", with the apex of the "V" corresponding to the closest point of approach by the seismic vessel. Western points were farther from the seismic survey area and received lower levels of sound exposure.

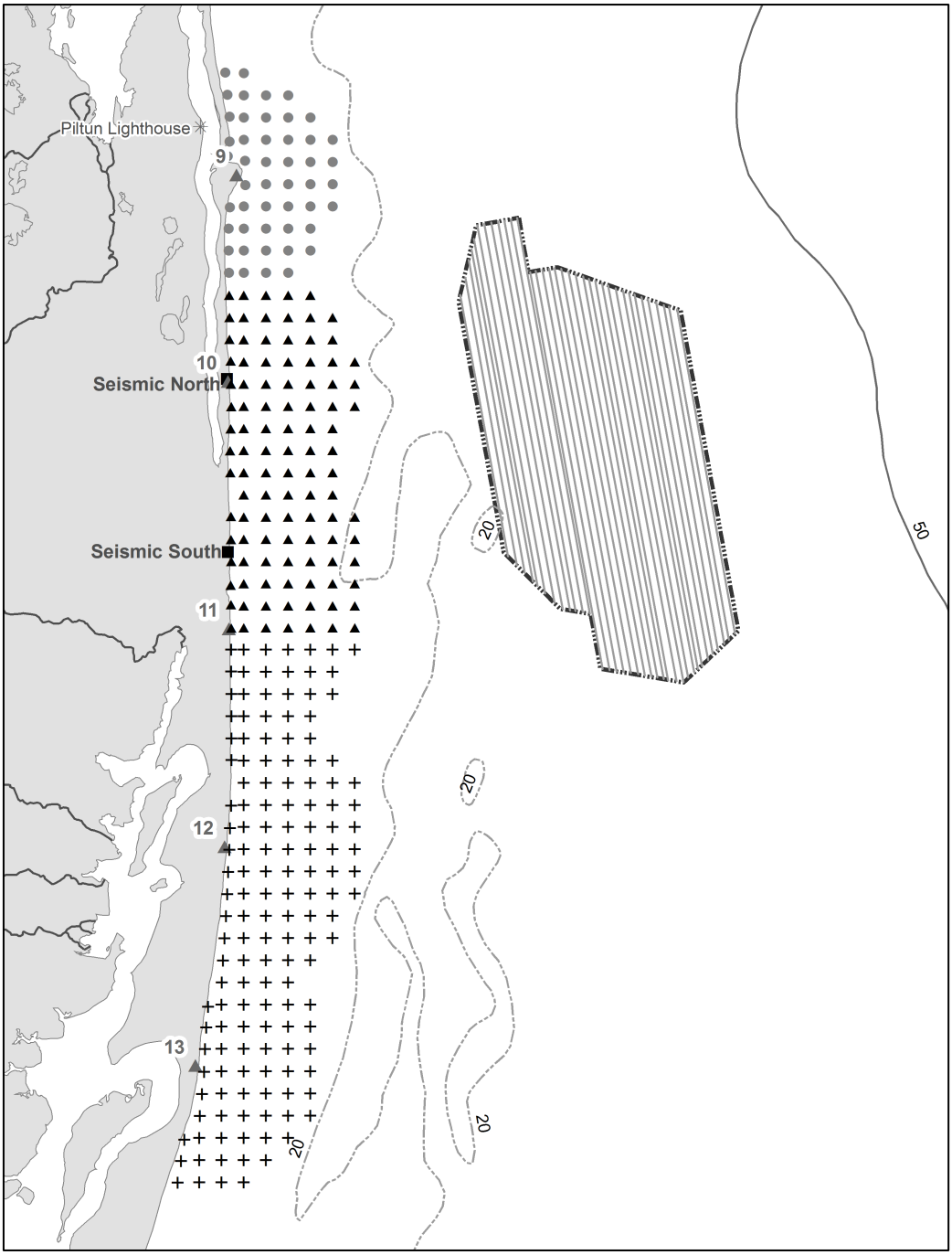

Fig. S3. Ensonification pattern categories. Black triangles correspond to grid cell centroids adjacent to seismic lines that will experience an inverted "V" in the sound pattern as the seismic vessel passes the grid cell. The gray circles and black crosses represent two areas of grid cell centroids with opposite monotonic patterns in sound levels during the shooting of a seismic line.

LITERATURE CITED

Ramsay JO, Silverman BW (2005) Functional Data Analysis 2nd edition. Springer, New York, NY

Supplement 3: The information contained in this Supplement provides details of methods and results for determination of the temporal blocking period used in model development.

Methods

The survey level density surfaces provided multiple snapshots of gray whale distribution and abundance at a fine temporal scale for analysis within each day of survey effort. However, a survey's density surface's coverage was often incomplete because poor weather (i.e., high winds, precipitation, fog) prevented scans at one or more stations during a survey. A distribution station was also occasionally skipped to keep surveys synchronized with seismic activity, and behaviour scans were not conducted when teams were engaged in focal observations at the scheduled scan time. These incomplete density surfaces had the potential to create spurious effects in the models. A second difficulty was the low proportion of non-zero density cells due to the primary mitigation of conducting the seismic survey when gray whale numbers were initially low, with the resulting potential for very wide confidence intervals on estimated covariate effects. While zero-inflated models can address many difficulties encountered with excess zero counts, they often have trouble identifying important covariates in the presence of extreme incidence of zeros (more than ~ 80%) (Ghosh et al. 2012).

We used temporal blocking to address these challenges of insufficient map coverage and low proportions of non-zero densities per surface. We initially averaged density surfaces for pairs of adjacent surveys within a day. We retained the remaining survey level density surface on days with odd numbers of surveys. The "adjacent survey" temporal scale did not improve coverage and numbers of non-zero densities sufficiently, and we expanded the temporal scale to test daily average density surfaces. These provided estimates for nearly all grid cells in the map coverage, and substantially increased the number of non-zero grid cells per surface. We therefore used daily surfaces in our main analysis. However, we conducted an extensive exploratory analysis on both the survey level and daily density surfaces prior to modelling to ensure important relationships were not being lost by using daily averages (see Supplement 4).

Results

The proportion of non-zero density cells ranged from a mean of 1.9 % for survey level density surfaces to 5.4 % in the daily surfaces (Table S1). The daily temporal scale had sufficient sampling effort within each time block to provide density estimates for all grid cells in the map coverage. Daily blocking also substantially increased the number of non-zero grid cells per temporal block compared to the other temporal scales.

Table S1. Summary of map coverage and density values for the survey level, adjacent survey and daily temporal blocking.

Temporal Block	Number of blocks	Block coverage (%)				Proportion non-zero grid cells			
		Mean	SD	Min	Max	Mean	SD	Min	Max
Survey	42	83.8	21.33	18.1	100	1.9	1.39	0	5.7
Adjacent surveys	24	88.8	22.81	18.1	100	2.8	1.98	0	6.6
Daily	10	98.7	1.71	95.7	100	5.4	3.03	1.0	10.4

LITERATURE CITED

Ghosh S, Gelfand A, Zhu K, Clark J (2012) The k-zig flexible modeling for zero-inflated counts. Biometrics 68(3): 878-885

Supplement 4: The information contained in this Supplement provides details of methods and results of preliminary model development that determined covariates of interest for the Bayesian occupancy and abundance models.

Methods

We conducted an initial stage of model development ("preliminary models") using the survey and daily level densities (see Supplement 3 "Temporal Blocking" for details of methods and results of analyses used to determine a temporal scale for the main modelling). Only two-part zero-inflated models were used in preliminary modelling because the independent parts were easier to fit and interpret compared to mixture models. These preliminary models did not include all random effects that account for repeated measurements and spatial correlation so that the models could be run using standard functions in R (R Development Core Team 2012). This approach allowed us to quickly test several candidate models at both the survey and daily level temporal scales. Although not optimal, these analyses provided an assessment of covariate effects, both singly and in combination, to inform development of the main models.

Generalized linear models (McCullagh & Nelder 1989) and linear mixed effects models (Zuur et al. 2010) were used for occupancy and abundance regressions respectively. Akaike Information Criteria (AICs) were used for model selection. As a sensitivity test, we subsetted data to exclude the three most easterly (farthest from shore) columns of grid cells, and repeated the modelling. This was to ensure results were not an artefact of gray whale natural occurrence closer to shore and the trend for increasing cumulative sound levels with increasing distance from shore for the longer 3 d and 7 d time windows. We explored spatial correlation by constructing variograms for all log densities, occupancy data and the positive density data at each temporal scale.

The survey and daily level results were compared for consistency to ensure important relationships were not being lost by using daily averages, and covariates of interest identified for the Bayesian hierarchical models.

Results

The same covariates were selected for survey and daily density surfaces in each of the occupancy and abundance final models, indicating important relationships between covariates and gray whale responses at the survey level were not lost by daily averaging. All models included Northing and an interaction between Easting and Depth. Day category was included for occupancy but not abundance. No detection covariates were retained. Of the sound covariates tested, only ensonification level category (EnsonLev) was retained for the occupancy model. The best model for abundance included a sound covariates for 3 d time windows with 3 d 24–hr FPC score 3 (3d24PC3).

The covariates selected for the Bayesian occupancy model included EnsonLev, Day, Northing and an interaction between Easting and Depth. Covariates for the Bayesian abundance model were 3d24PC3, Northing and an interaction between Easting and Depth.

The occupancy and abundance models run on the subset of eastings (X_UTM_KM) were similar to those using the entire data set.

LITERATURE CITED

McCullagh P, Nelder JA (1989) Generalized linear models 2nd Edition. Chapman & Hall/CRC monographs on statistics and applied probability 37. Boca Raton, FL

R Development Core Team (2012) R: A language and environment for statistical computing. R Foundation for Statistical Computing, Vienna, AT

Zuur AF, Ieno EN, Walker NJ, Saveliev AA, Smith GM (2010) Mixed effects models and extensions in ecology with R. Springer, New York, NY